Organic & Biomolecular Chemistry

Molecular Tetrominoes: Selective Masking of Donor pi-face to Control Configuration of Donor-Acceptor Complex

Journal:	*Organic & Biomolecular Chemistry*
Manuscript ID	OB-ART-11-2021-002293
Article Type:	Paper
Date Submitted by the Author:	23-Nov-2021
Complete List of Authors:	Sartucci, Jenna; Georgetown University, Chemistry Maity, Arindam; Georgetown University, Chemistry Mohanan, Manikandan; Georgetown University, Chemistry Bertke, Jeffery; Georgetown University, Department of Chemistry Kertesz, Miklos; Georgetown University, Department of Chemistry Gavvalapalli, Nagarjuna; Georgetown University, Chemistry

SCHOLARONE™
Manuscripts

Molecular Tetrominoes: Selective Masking of Donor π-Face to Control Configuration of Donor-Acceptor Complex

Jenna L. Sartucci,[a,b] Arindam Maity,[a,b,†] Manikandan Mohanan,[a,b,†] Jeffery Bertke,[a] Miklos Kertesz,[a,b] and Nagarjuna Gavvalapalli[a,b]*

[a]*Department of Chemistry and* [b]*Institute for Soft Matter Synthesis and Metrology, Georgetown University, 3700 O St NW, Washington, D.C., 20057, USA.*

Abstract

Understanding the doping mechanism in organic semiconductors and generating molecular design rules to control the doping process is crucial to improve the performance of organic electronics. Even though controlling the location and orientation of the dopant along the semiconductor backbone is an important step in the doping mechanism, studies in this direction are scarce as it is a challenging task. To address this, here in, we incorporated π-face masked (strapped) units in 1,4-bis(phenylethynylene)benzene (donor) to control the acceptor (dopant) location along the trimer, donor-acceptor binding strength, and acceptor ionization. Two strapped trimers, PCP and CPC, are synthesized with control over the location of the strapped repeat unit in the trimer. The trimers are complexed with 2,3-Dichloro-5,6-dicyano-1,4-benzoquinone (DDQ) acceptor in solution. DFT calculations show that DDQ residing on the non-strapped repeat unit (percentage of this configuration is at least ca. 73%) has the highest binding energy for both PCP and CPC. The percentage of dopant ionization is higher in the case of strapped trimers (PCP and CPC) compared to that of linear control trimers (PLP and LPL) and completely non-strapped (PPP) trimer. The percentage of dopant ionization increased by 15 and 59% in the case of PCP and CPC respectively compared to that of the PPP.

Introduction

Understanding the doping mechanism in organic semiconductors and generating molecular design rules to control the doping process has been an active research area for the past few decades.[1-5] The research in this direction has rejuvenated recently and gained momentum with the increased interest toward organic thermoelectrics.[6-15] Thermoelectric performance of an organic semiconductor depends on its electrical conductivity, and molecular doping is one of the common strategies employed to increase the conductivity, hence the thermoelectric performance. The molecular doping process commonly involves mixing an electron rich (poor) organic semiconductor with an electron deficient (rich) molecule commonly referred to as dopant. A
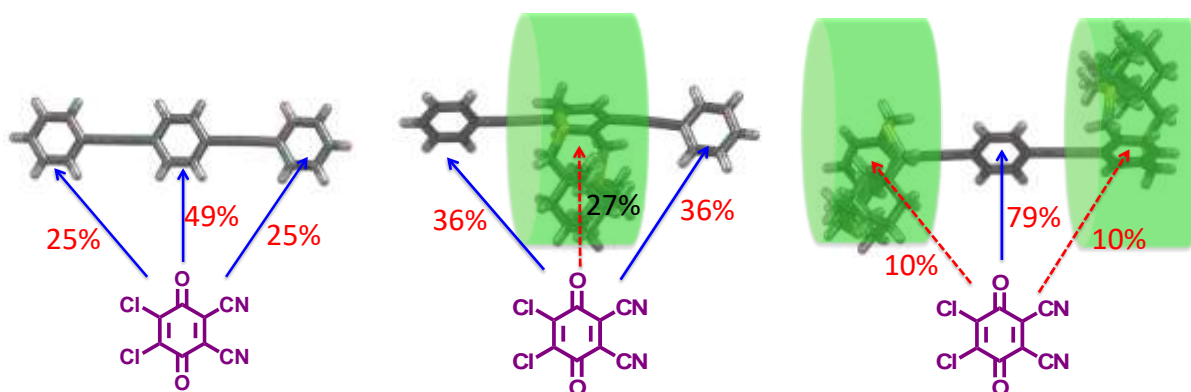

Scheme 1. Three donor-acceptor pairs studied in this work. DDQ complex with (left) non-strapped donor (PPP); (middle) middle repeat unit strapped donor (PCP); (right) terminal repeat units strapped donor (CPC). Green color cylinder is shown around cyclophane to indicate rotation of the cyclophane unit create an insulating sheath. The insulating sheath reduces the interaction of acceptor with the cyclophane phenyl compared to non-strapped phenyls. Blue and red color arrows indicate most and least accessible locations for DDQ along the trimer backbone. Percentage configuration of DDQ residing on each of the units is determined using DFT (*vide infra*) calculations and is shown on the arrow.

charge transfer from the semiconductor to the dopant generates ionized species, which will help to enhance the electrical conductivity and thermoelectric performance. Thus, it is crucial to pair a semiconductor with the appropriate dopant to achieve maximum ionization of the dopant.

Several organic semiconductors including π-conjugated polymers, oligomers and small molecules as well as dopants have been studied to understand the key structural factors that play an important role in dopant ionization and the electrical conductivity. [6-15] Unlike the small molecule hosts, in the case of oligomer and polymer hosts several binding sites are available for dopants to bind. Location and orientation of the dopant along the polymer backbone along with distance between the doping sites play a crucial role in determining the doping efficiency and conductivity. Recently, Kim and coworkers have shown that for a donor-acceptor copolymer the dopant binding strength varies depending on its location on the backbone i.e., the repeat unit with which it is interacting.[16] Even though controlling the location and orientation of the dopant along the polymer backbone is an important step in the doping mechanism, studies in this direction are scarce in the literature as it is a challenging task to realize.

Several research groups including our research group has shown that molecular sheathing of a π-conjugated polymer backbone masks the conjugated backbone and hinders interchain interactions.[17-31] We have shown that cycloalkyl straps not only reduce interchain interactions but also reduce photoinduced charge transfer from conjugated polymer backbone to acceptor molecules. This has resulted in a reduction of the Stern-Volmer quenching constant of the cycloalkyl strapped polymers compared to conventional π-conjugated polymers with pendant solubilizing chains.[17, 31] Even though the cycloalkyl straps are only masking one of the π-faces of the repeat unit, the free rotation of the repeat unit around the polymer axis generates a cylindrical insulating sheath around the polymer backbone. The insulating sheath is expected to reduce the interaction of acceptor with the cyclophane unit. This prompted us to use the cycloalkyl strap containing repeat units to control the binding interactions with dopants as well as ionization of dopants.

In order to control the binding strength and location of the dopant along the oligomer backbone, herein we designed and synthesized PCP (phenyl-cyclophane-phenyl) and CPC (cyclophane-phenyl-cyclophane), two strapped 1,4-bis(phenylethynylene)benzene molecules, here on called as strapped trimers (Scheme 1). In the PCP the cycloalkyl strapped phenyl repeat unit is in the middle whereas in the CPC the strapped phenyl repeat units are at the terminal. A PPP (phenyl-phenyl-phenyl) trimer that has no strapped phenyls and two donor trimers (PLP [phenyl-linear-phenyl] and LPL [linear-phenyl-linear] also called as linear-trimers) analogous to the PCP and CPC but with the linear substituents are synthesized as control trimers and studied for comparison. All five trimers (donors) are complexed with 2,3-Dichloro-5,6-dicyano-1,4-benzoquinone (DDQ) acceptor (dopant) in solution. The percentage of dopant ionization is higher in the case of strapped trimers (PCP and CPC) compared to the non-strapped trimer (PPP)
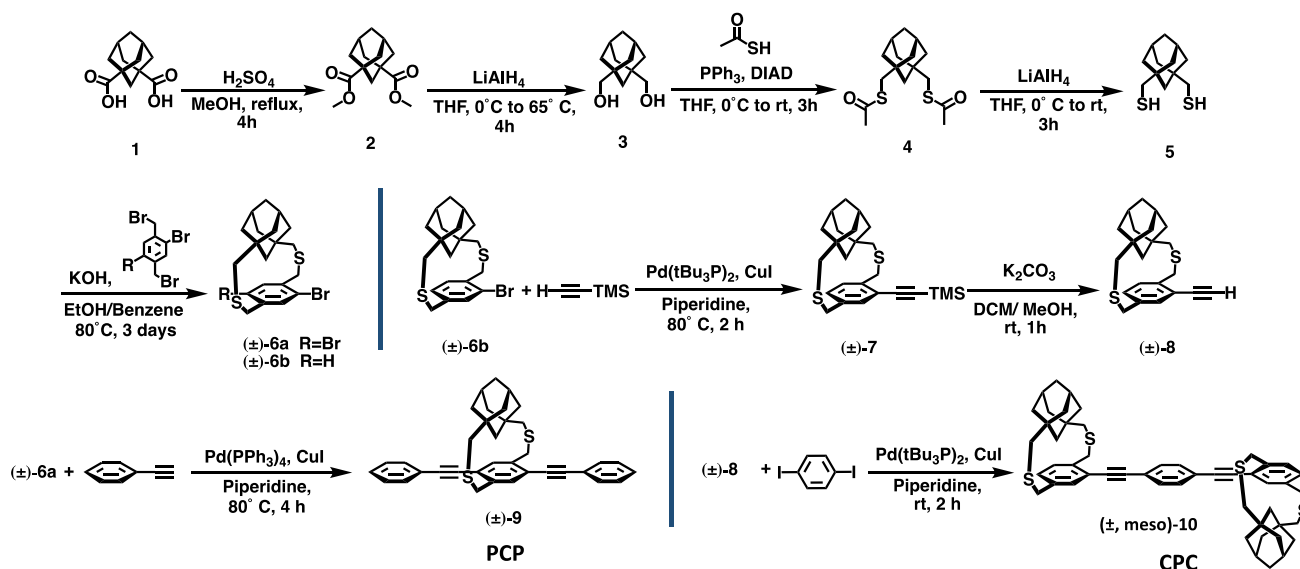

Scheme 2. Scheme for the synthesis of Donors **(±)9** (PCP) and **(±, meso)-10** (CPC) and their precursors.

and linear trimers (PLP and LPL). The percentage of dopant ionization increased by 15 and 59% in the case of PCP and CPC respectively compared to that of the PPP. DFT calculations have shown that binding energy of DDQ with both CPC and PCP are the same and higher than that of

PPP. Also, DDQ residing on the non-strapped repeat unit is the highest percentage configuration (ca. 74%) and is the lowest energy (highest binding energy) configuration for both the strapped trimmers, supporting our hypothesis that by masking donor-repeat units of the donor-acceptor complex, the configuration can be controlled.

Experimental

All chemicals were used as purchased unless otherwise stated. The donor PPP and acceptor DDQ as well as 1,3-adamantane dicarboxylic acid were purchased from Sigma Aldrich, Alfa Aesar, Oakwood Chemical, or AK Scientific. The strapped trimers are synthesized following Scheme 2. Linear trimers are synthesized following Scheme S1 and S2 as shown in supporting information. Samples for UV-Vis spectroscopy of individual trimer and acceptor molecules were prepared in chloroform at a concentration of 10 μM and spectra were measured at room temperature. Complexes were made by mixing separate solutions of donor and acceptor in chloroform (or tetrahydrofuran [THF] as stated) at room temperature so that final solutions were 5 mM in each donor and acceptor. Samples for ATR-IR were prepped in chloroform and were dried by a stream of nitrogen followed by high vacuum.

Computational methods: All computations were done by the Gaussian 16 package.[32] The individual trimers as well as DA configurations were optimized using density functional theory (DFT) at the
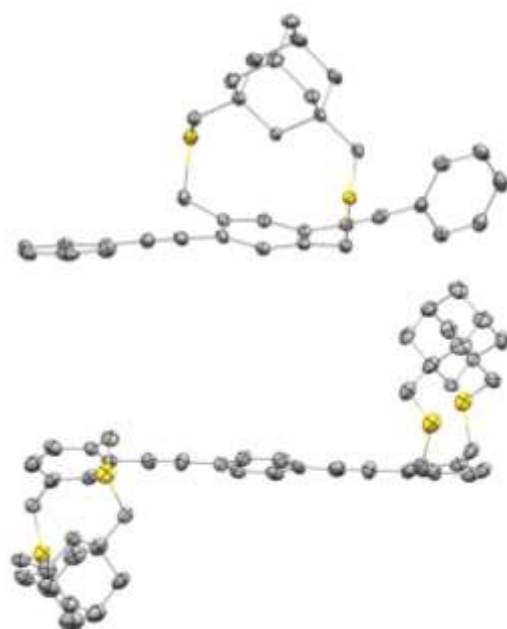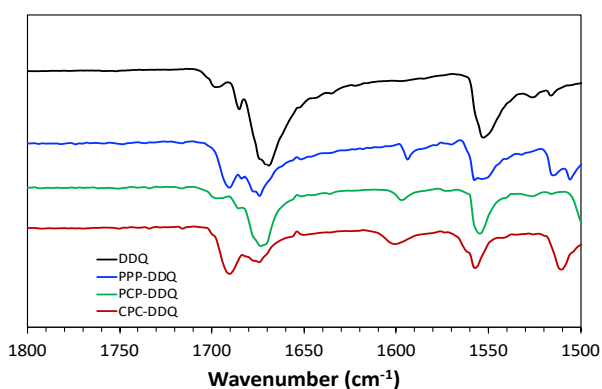

Figure 1. Single crystal X-ray thermal ellipsoid plots of (top) PCP ((±)-**9**) and (bottom) CPC ((±)-**10**) with thermal ellipsoids at 50% probability. Gray-C, yellow-S (hydrogens are omitted for clarity).

B3LYP/6-311G** level. A dispersion correction was added with GD3BJ. All local minima were confirmed by obtaining only real vibrational frequencies. Time-Dependent Density Functional Theory (TD-DFT) was used to gain insight on the effect of DA configuration on the position of the charge transfer peak in the absorption spectra for all three charge transfer complexes. A long-range corrected functional using the Coulomb attenuating method (CAM-B3LYP/6-311G** with added dispersion GD3BJ) [33-34] was used for TD-DFT using the B3LYP/6-311G** optimized geometries. Coordinates of optimized geometries are provided in the Supporting Information section.

Results and Discussion

In order to control the location of the DDQ along the 1,4-bis(phenylethynylene)benzene backbone, two adamantyl strapped 1,4-bis(phenylethynylene)benzene molecules, PCP and CPC, are synthesized. In the PCP the adamantyl strap is on the middle phenyl unit whereas in the CPC the adamantyl strap is on both the terminal phenyls. The adamantyl group masks the π-face of the phenyl and reduces the possibility of the DDQ to interact face-to-face on that side of the repeat unit. Also, the free rotation of the phenyl repeat unit around the trimer long axis forms an insulating sheath around the adamantyl containing repeat unit (Scheme 1). The insulating sheath reduces the possibility of DDQ to bind from the unmasked side of the cyclophane as well, thus overall reducing the binding energy with adamantyl-strapped repeat unit. This will enhance the binding of the DDQ at the non-strapped repeat units

Figure 2. ATR-IR spectra of charge transfer complexes prepared from chloroform solution.

and provides a pathway to control the location of the acceptor along the trimer backbone.

The PCP and CPC donors are synthesized as shown in Scheme 2. Sonogashira coupling of (±)-6a with phenylacetylene gave PCP in 66% yield. Sonogashira coupling of (±)-8 with 1,4-diiodobenzene gave CPC with 69% yield. The adamantanocyclophane precursors (±)-6 through (±)-8 are synthesized following our previous reports.[17, 35] The racemic adamantanocyclophanes are used in further steps without chiral resolution hence the PCP is a racemic mixture and CPC is a mixture of enantiomers and meso compounds. The structure of the synthesized donors PCP ((±)-9) and CPC ((±, meso)-10) were confirmed through NMR and single crystal X-Ray crystallography. PCP crystallized from chloroform into an orthorhombic crystal with the space group $P2_12_12_1$ and CPC crystallized from chloroform into a triclinic crystal system with the space group P-1 (Figure 1 and Table S1).

Donor-acceptor (DA) complexes were made by mixing separate solutions of donor and acceptor (1:1 ratio) in chloroform at room temperature. Concentrations of the donor and acceptor in the complex are 5 mM each. DA complexes are characterized using ATR-IR and UV-Vis absorption spectroscopy. The samples for FTIR are dried using a stream of nitrogen followed by high vacuum and are analyzed using ATR-IR (Figure 2 and Figure S1). Charge transferred to DDQ delocalizes over the carbonyls and alters their stretching frequency. Therefore, DDQ's carbonyl stretch is used as a characteristic peak to study and confirm the DA complex formation in the literature.[36-39] In the case of aryl thiols, complexes with
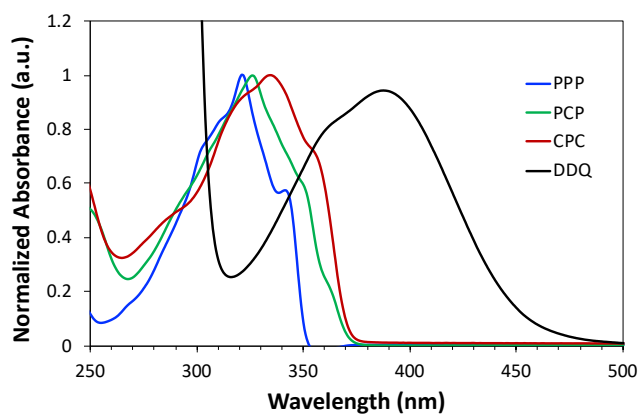
Figure 3. Normalized UV-vis absorbance spectra of trimers and DDQ in chloroform.

DDQ show a shift in the frequency of the C=O stretch compared to pristine DDQ, confirming the complex formation between the aryl thiols and DDQ.[39] Similar to that, DDQ's carbonyl stretch is shifted by ca. 5 cm^{-1} and appears at ca. 1675 cm^{-1} in all three complexes made with the trimers, indicating the formation of DA complex. In addition to the shift, there is also a change in the intensity of the 1690 cm^{-1} peak relative to the 1675 cm^{-1} peak indicating that the carbonyl has different chemical environment in all three complexes due to the difference in the donor architecture and DA configuration (vide infra).
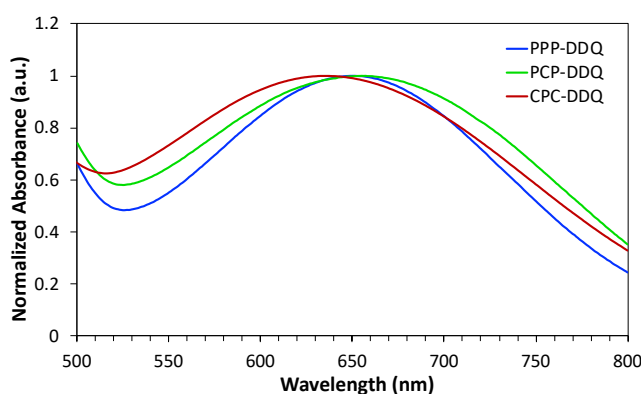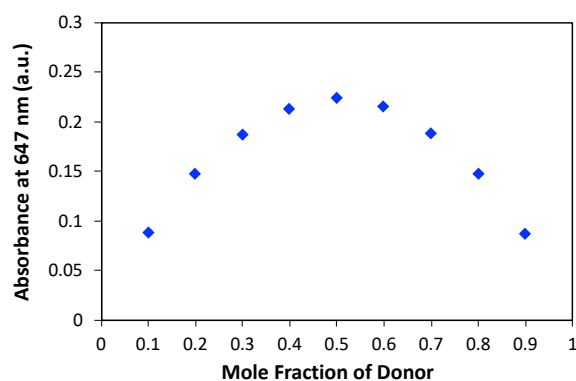

Figure 4. Normalized UV-vis absorption spectra of the charge transfer complexes in chloroform (only charge transfer peak is shown for clarity).

Next, to determine the impact of strapped-repeat units on DA complex formation, UV-Vis absorption spectra of the DA complexes were recorded. The absorption spectra of the donors, DDQ and DA complexes are shown in Figures 3 and 4. The absorption maximum of the trimers increases by a few nm as the strapped-repeat units replace the phenyl groups. The PPP donor has an absorption maximum ca. 324 nm whereas the CPC donor has an absorption maximum ca. 337 nm. Also, the shoulder peak position red shifts and the intensity increases as the number of strapped-repeat units increase in the donor. The absorption edge for both the strapped trimers (PCP and CPC) is 20 nm red shifted compared to that of PPP donor, indicating that their optical


Figure 5. Job's Plot for the PPP-DDQ charge transfer complexation in chloroform.

band gap is ca. 0.2 eV lower than that of unstrapped PPP. DDQ has a λ_{max} ca. 390 nm with strong absorption below 300 nm.

The absorption spectrum of the three DA complexes in chloroform is shown in Figure 4 and Figure S2. All three DA complexes show a new absorption peak in the visible region (ca. 650 nm), which is not present in the either the donors or acceptor at this concentration indicating that this peak is due to a charge transfer interaction between donor and acceptor. Previously it has been shown that *p*-terphenyl, three phenyls connected without a spacer, shows a charge transfer peak at ca. 635 nm with DDQ.[40] Thus, the peak ca. 650 nm in all three DA complexes is assigned as the charge transfer peak. Since each trimer contains three aryl groups there is a possibility for each trimer to complex with more than one DDQ. In order to find the stoichiometry of the DA complexes, the formation of DA complex was analyzed using the method of continuous variation (Job's Plot). Job's plots are shown in Figure 5 and Figures S3 and S4. For all three donors, the absorbance of the charge transfer peak is largest at the equal ratio of donor and acceptor, indicating that in all three trimers the DA complex is indeed a 1:1 complex.

The absorption maximum of the charge transfer peaks showed no clear trend, unlike the absorption maximum of individual donors. The absorption maximum of the charge transfer peak for the PPP-DDQ complex is ca. 650 nm, whereas for the PCP-DDQ complex the charge transfer peak is red shifted about 10 nm. In contrast, the charge transfer peak for
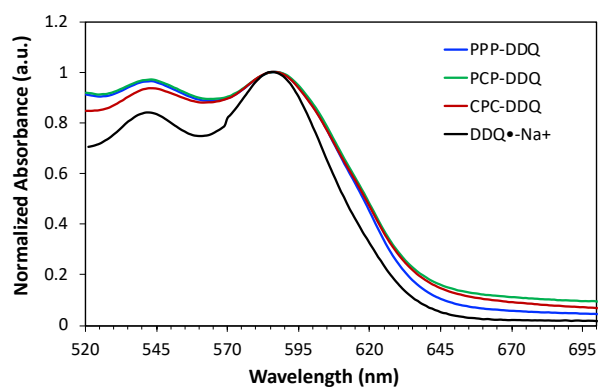
Figure 6. Normalized UV-Vis absorption spectra of charge-transfer complexes in tetrahydrofuran.

the CPC-DDQ complex is blue shifted by 20 nm. The difference in the absorption maximum of charge transfer peak is attributed to the difference in DA configuration of each DA complex, which is further due to the presence of strapped-repeat units in donors.

All three DA pairs exist as DA complex in chloroform, a non-polar solvent, and it is known that DA complexes dissociate into ionic complexes in polar solvents.[41] In order to understand the impact of selectively masking the π-face of a few repeat units along the trimer on acceptor ionization, the DA complexes are synthesized in THF- a polar solvent. In THF all the three DA pairs show no absorption peaks ca. 650 nm but instead show two new peaks ca. 545 and 590 nm (Figure 6 and Figure S5). This peak pattern is in reminiscent of the DDQ radical anion absorption spectrum.[39, 42-43] Indeed, the absorption spectrum of chemically reduced DDQ (using NaI) in THF showed absorption peaks at ca. 545 and 585 nm. This suggests that all three DA pairs exist as DA complex in chloroform (a less-polar solvent) whilst they exist as charge separated species in THF (a more polar solvent). The polar nature of the THF solvent helps to stabilize the charge separated state that result in ionic species, as previously shown in the literature for other DA complexes.[44] More importantly, the absorbance of the DDQ radical anion species increases as the number of strapped repeat units increases in the donor. The percent increase in DDQ ionization in strapped DA complexes relative to PPP-DDQ complex is determined using the equation shown in supporting
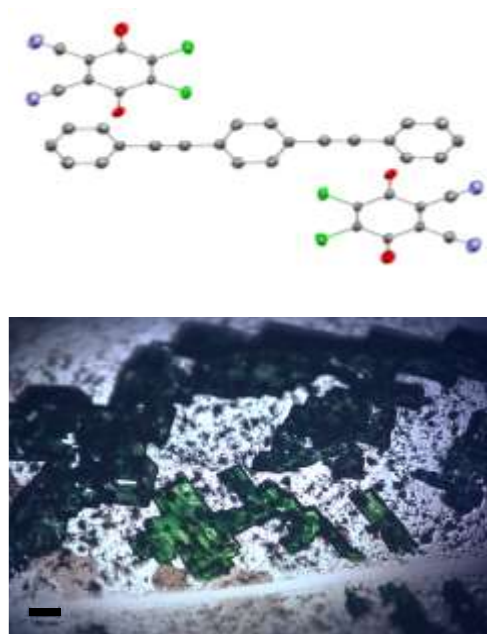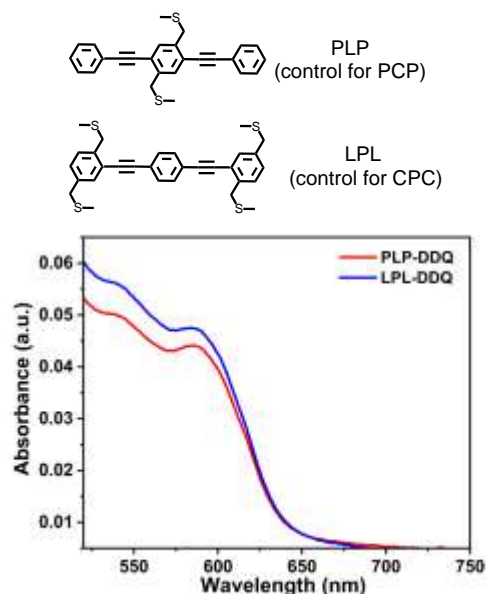

Figure 7. Single crystal X-ray thermal ellipsoid plots (top) and photograph (bottom) of PPP-DDQ charge transfer complex crystal. Thermal ellipsoids at 50% probability. Gray-C, red-O, green-Cl, blue-N (hydrogens are omitted for clarity). Scalebar is 100 μm.

information. The concentration of the DDQ radical anion increased by 15% and 59% when PCP and CPC are used as donors compared to PPP donor (Figure S5). The difference in dopant ionization could be due to the difference in the frontier energy levels.

Two probe this, two control donor trimers (PLP and LPL also called as linear-trimers) analogous to the PCP and CPC but with the linear substituents are synthesized (Figure 8 and see Supplementary Information). Both PLP and LPL contain alkylthioether substituents in the place of adamantyl thioether substituents to keep the electronic nature of the strapped and the corresponding linear trimers the same. PLP and LPL are synthesized from commercially available molecules in a couple of steps as shown in the supporting information. Linear-trimer and DDQ complexes are prepared following the similar procedure discussed above. Both complexes showed a shift in the DDQ's carbonyl stretch indicating the formation of DA complex (Figure S6). PLP and LPL have absorption similar to that of PCP. The Job's plot

Figure 8. (top) Chemical structures of linear control trimers, PLP and LPL; (bottom) non-normalized UV-vis absorption spectra of PLP-DDQ and LPL-DDQ complexes in tetrahydrofuran.

of linear-trimers with DDQ confirms that both the complexes are formed in 1:1 ratio (Figure S6). PLP complex showed a charge transfer peak at 650 nm similar to that of the PCP complex. On the other hand LPL complex showed a broad charge transfer peak with maximum at 585 nm and a shoulder at 680 nm (Figure S6). LPL-DDQ complex ATR-IR showed a broad peak for carbonyl with a maximum at 1690 cm^{-1} (Figure S6). ATR-IR and UV-vis studies indicate that the LPL complexes differ in configuration and/or strength of complexation compared to rest of the

complexes. UV-vis spectra of both PLP and LPL complexes in THF showed peaks that are reminiscent of DDQ$^-$ and the absorbance of this peak at 550 nm is used to determine the percentage DDQ ionization (Figure 8). Both the complexes showed relatively lower percentage (smaller by 15-20%) of DDQ ionization compared to PPP control complex. A direct comparison of linear trimer complexes with the analogous strapped trimer complexes show that strapped trimers result in higher percentage of DDQ ionization, 50% increase in the case of PLP to PCP and 80% increase in the case of LPL to CPC. Since the electronic structure of the substituents on the linear trimers and the bridges in the strapped trimers are similar, the increase in DDQ ionization from PPP to strapped trimers is attributed to the adamantyl straps and their location along the trimer. The adamantyl straps alter the configuration and strength of the trimer-DDQ complex resulting in higher DDQ ionization.

Cyclic voltammetry of trimers was not successful (Figure S11). The frontier energy levels of the strapped trimers are estimated from the optical transitions of individual donors and charge transfer complexes together. The LUMO energy of the DDQ is reported to be at -4.3 eV.[45-46] The charge transfer peak in the DA complexes is due to the electronic transition from HOMO of the trimer to the LUMO of DDQ. The HOMO energies of the trimers are determined by combining the charge transfer transition value and the LUMO energy of the DDQ (Table S2). The optical properties of the individual trimers and DA complexes as well as the trimers' frontier energy levels are comparable, thus the difference in dopant ionization is attributed to the difference in DA configuration.

In order to determine the location of DDQ along the donor backbone, attempts were made to grow single crystal structures of DA complexes. Out of three complexes, only the PPP-DDQ complex resulted in a cocrystal. The cocrystal is slightly disordered and exhibited a bright

green color similar to that of the charge transfer complexes in solution (Figure 7). The cocrystal is a triclinic system and has a P-1 space group. The molecules pack in a ratio of 1:2 PhPhPh to DDQ and have a π-π stacking distance of 3.35 Å. PPP and DDQ crystallize in a 1:2 ratio although the solution contains an equimolar mixture of both the components. This difference in component composition between solution and single crystals is previously observed in DA systems and depends on various factors including solvent, growth time, temperature, binding strength, and packing efficiency.[47-48] Interestingly, in the cocrystal, the lengths of specific bonds changed relative to the lengths of neutral DDQ. In this case, the length of C-C bond between carbonyl carbon to the carbons with -Cl or -CN substituents shortened by 0.007 to 0.018 Å and only a slight increase (0.002 to 0.005Å) in the C=O bond length is observed. As expected, the change in bond lengths is relatively small compared to the bond length changes observed from DDQ to DDQ radical anion, indicating a partial charge transfer has occurred in the complex.[49-53] Many attempts were made to grow cocrystals of the strapped trimers (PCP and CPC) with DDQ but unfortunately, all attempts were futile. The racemic nature of the strapped trimers along with the possibility of having various DA complex configurations makes it difficult for them to co-crystalize.

DFT calculations were used to gain insights on the role of having strapped repeat units at different locations along the trimer backbone on the location of the DDQ along the donor backbone as well as DA binding strength. The presence of strapped-repeat units on the trimer reduces the symmetry of the trimer and makes some of the DDQ complexation locations on the trimer non-degenerate, increasing the number of possible DA configurations. In addition to this, the conformation of the trimer as well as orientation of the DDQ along the trimer can be varied. Thus, the number of possible DA configurations is higher for strapped trimers compared to

14

unstrapped PPP. PPP-DDQ complexes are optimized by placing the DDQ on the central and

terminal phenyl ring (Figure 9). In addition, orientation of the DDQ on the PPP is also varied by

keeping the carbonyls either along or orthogonal to the PPP long axis. The four key optimized

a)

PPP-DDQ-1

b)

PPP-DDQ-2

c)

PPP-DDQ-3

d)
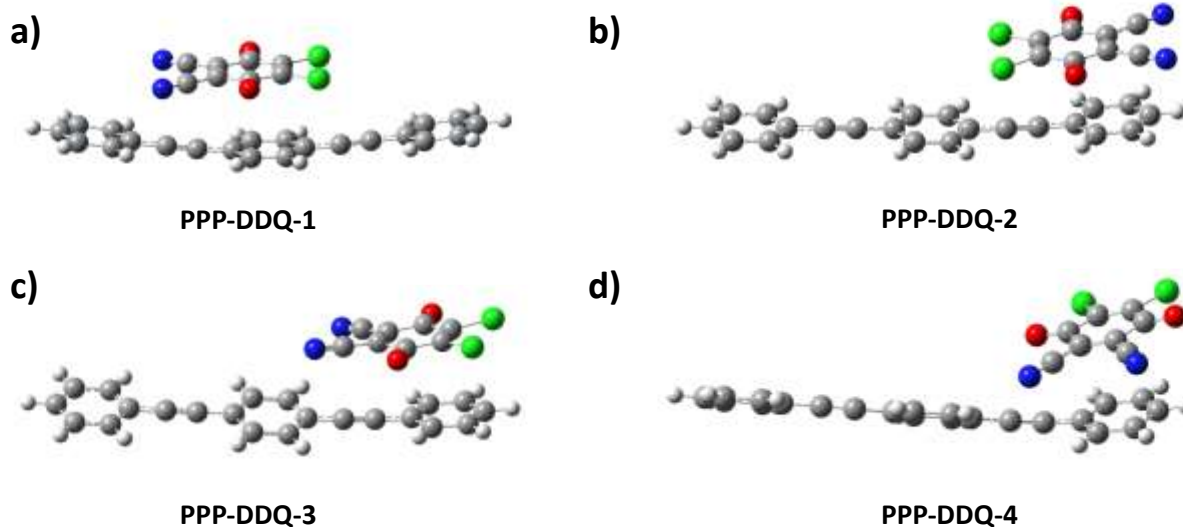
PPP-DDQ-4

Figure 9. Four key configurations of PPP-DDQ that are optimized with DFT-B3LYP/6-311G**
calculations.

configurations for PPP-DDQ complex are shown in Figure 9. Binding energies for each of these

configurations was calculated and are shown in Table 1. The relative binding energy i.e., the

difference in binding energy of a configuration compared to the most stable configuration is also

shown in Table 1. The Boltzmann factor is also calculated for each configuration and is used to

determine the percentage of each configuration. The PPP-DDQ-1 configuration where the DDQ

Table 1. Binding energy and optical transitions of optimized PPP-DDQ charge transfer configurations.

System	BE ^{a} (kcal/mol)	$\Delta BE_r{}^b$ (kcal/mol)	BF ^{c}	% Configuration	$\lambda_{CT}{}^d$ (nm)	$f_w{}^e$
PPP-DDQ-1	19.29	0	2	49 %	No peak	--
PPP-DDQ-2	18.6	0.69	1.27	31 %	No peak	--
PPP-DDQ-3	18.28	1.01	0.66	16 %	759	0.023
PPP-DDQ-4	17.41	1.88	0.17	4 %	658	0.018

^{a}BE (binding energy, BE= -($E_{complex}$- E_{donor}- E_{DDQ}); $^b\Delta BE_r$: relative binding energy (ΔBE_r=BE (most stable configuration)- BE(complex)); ^{c}BF: Boltzman factor (BF= g*e$^{-\Delta BEr/RT}$ where g describes the degeneracy of each energy level; ΔBE_r: relative binding energy of the complex); $^d\lambda_{CT}$: Calculated charge transfer transition; $^e f_w$ weighted oscillator strength: BF x calculated oscillator strength.

is located over the top of central phenyl ring with carbonyls orthogonal to the donor axis (Figure

9a) has the highest computed binding energy and its percentage in the composition is ca. 49%.

The simulated PPP-DDQ-2 configuration, a configuration similar to that of the single crystal X-

ray structure, has lower computed binding energy than the PPP-DDQ-1 by ca.1 kcal/mol

nonetheless; it exists ca. 31% in the composition. The DA configuration in simulations is driven

a)   b)   c)

PPP-DDQ   PCP-DDQ   CPC-DDQ
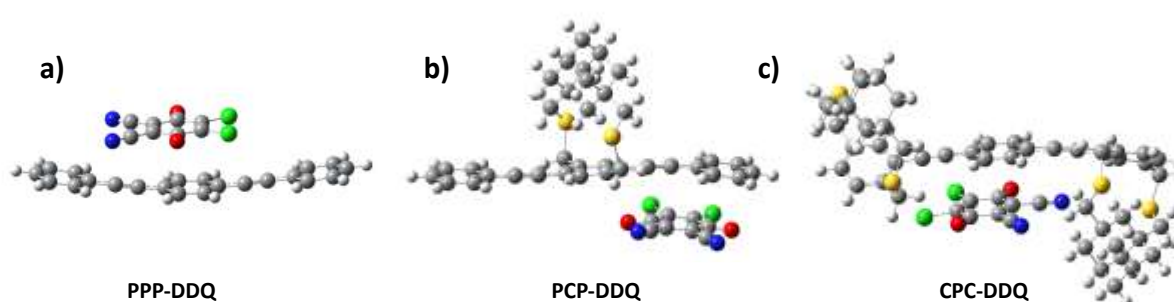
Figure 10. DA configurations having highest binding energy for each DA complex.

by the maximum interaction and binding energy. On the other hand, in the single crystal

structure the configuration is determined by the packing efficiency in addition to the binding

energy.

The binding energy and DA configuration for strapped trimers are also determined following a similar protocol as discussed above. The key difference in the case of PCP and CPC trimers is that more configurations are optimized as the number of possible locations and orientations increases due to reduced symmetry. For example, in the case of CPC either both the adamantyls can be on same side (U shape conformer) or they can be on opposite sides (Z shape conformer). The CPC crystallizes in the Z shape conformation but in solution it can access all the

Table 2. Binding energy and optical transitions of optimized PCP-DDQ charge transfer configurations

System	BE ^{a} (kcal/mol)	ΔBE_r ^{b} (kcal/mol)	BF ^{c}	% Configuration	λ_{CT} ^{d} (nm)	f_w ^{e}
PCP-DDQ-1	23.66	0	2	73 %	586, 489	0.366, 0.038
PCP-DDQ-2	23.48	0.18	0.74	27 %	728, 543, 487	0.0016, 0.038, 0.002
PCP-DDQ-3	19.71	3.95	0.002	< 0.1 %	675, 567	0, 0
PCP-DDQ-4	19.12	4.54	0.001	< 0.1 %	695, 567	0, 0
PCP-DDQ-5	19.08	4.58	0	-	644, 519	0, 0
PCP-DDQ-6	18.83	4.83	0.001	< 0.1 %	771, 551	0, 0
PCP-DDQ-7	17.63	6.03	0	-	None	None

^{a}BE (binding energy, BE= -(E$_{complex}$- E$_{donor}$- E$_{DDQ}$); $^b\Delta BE_r$: relative binding energy (ΔBE_r=BE (most stable configuration)- BE(complex)); ^{c}BF: Boltzman factor (BF= g*e$^{-\Delta BEr/RT}$ where g describes the degeneracy of each energy level; ΔBE_r: relative binding energy of the complex); $^d\lambda_{CT}$: Calculated charge transfer transition; $^e f_w$ weighted oscillator strength: BF x calculated oscillator strength.

possible conformations since the repeat units are linked through ethynyl linkers. Hence both the conformers of CPC are used to simulate various possible DA configurations. Simulated DA configurations of strapped trimers that show the highest computed binding energy (PCP-DDQ-1 and CPC-DDQ-1) are shown in Figure 10. Similar to the case of the PPP, there are other possible

DA configurations for both the strapped trimers with computed binding energies closer to the most stable configuration and these are shown in Figures S7 and S8. The relative binding energy, Boltzmann factor, and percent contribution for each configuration are calculated and are shown in Tables 2 and 3. Surprisingly, the binding energy for most stable configuration of both the

Table 3. Binding energy and optical transitions of optimized CPC-DDQ charge transfer configurations

System	BE ^{a} (kcal/mol)	ΔBE_r^b (kcal/mol)	BF ^{c}	% Configuration	λ_{CT}^d	f_w^e
CPC-DDQ-1	23.66	0	2	38 %	751, 563, 526	0.024, 0.001, 0.006
CPC-DDQ-2	23.63	0.03	1.9	36 %	720, 533, 508, 448	0.08, 0.01, 0.005, 0.02
CPC-DDQ-3	22.77	0.89	0.23	4 %	649, 512, 492	0.016, 0.002, 0.001
CPC-DDQ-4	22.6	1.06	0.36	7 %	640, 545, 466	0.002, 0.02, 0.001
CPC-DDQ-5	22.6	1.06	0.36	7 %	639, 557, 471	0.006, 0.016, 0.001
CPC-DDQ-6	22.45	1.21	0.27	5 %	640, 545	0.002, 0.014
CPC-DDQ-7	21.6	2.06	0.06	1 %	746, 576, 475	0.001, 0.002, 0.001
CPC-DDQ-8	21.44	2.22	0.05	1 %	742, 576, 475	0.001, 0.001, 0.001
CPC-DDQ-9	20.36	3.3	0.04	1 %	547	0
CPC-DDQ-10	20.18	3.48	0.06	1 %	646, 566	0.008, 0.0003
CPC-DDQ-11	14.93	8.73	0	-	635, 552, 493	0, 0, 0

^{a}BE (binding energy, BE= -(E$_{complex}$- E$_{donor}$- E$_{DDQ}$); $^b\Delta BE_r$: relative binding energy (ΔBE_r=BE (most stable configuration)- BE(complex)); ^{c}BF: Boltzman factor (BF= g*e$^{-\Delta BEr/RT}$ where g describes the degeneracy of each energy level; ΔBE_r: relative binding energy of the complex); $^d\lambda_{CT}$: Calculated charge transfer transition; $^e f_w$ weighted oscillator strength: BF x calculated oscillator strength.

strapped trimers is higher by 4 kcal/mol compared to PPP. Also, interestingly in both the highest computed binding energy configurations, the DDQ is on the unmasked-phenyl ring but not on the strapped-repeat units indicating that masking the π-face has a significant role in DA complex configuration as well as binding energy. Moreover, the percentage of the configurations where the DDQ is on the unmasked phenyl ring is at least 73% and 74% for PCP and CPC respectively,

clearly highlighting the DDQ's preference for unmasked phenyl groups along the strapped trimers backbone.

The adamantyl straps mask the π-face of the repeat unit and direct the DDQ toward the unstrapped repeat unit compared to the bare PPP. In order to determine if the substituents electronic nature has a role on directing the DDQ towards the unsubstituted repeat units the binding energies of the configurations of the complexes between
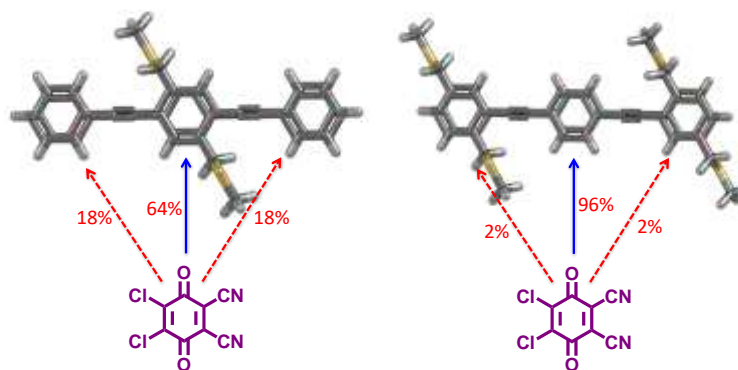

Scheme 3. Percentage of the weights of configuration of linear trimer-DDQ complexes wherein the DDQ is located on the middle or terminal repeat units. Blue and red color arrows indicate most and least accessible locations for DDQ along the trimer backbone.

linear trimers and DDQ are computed. Configuration and binding energies of the linear trimer-DDQ complexes are calculated by placing the DDQ on unsubstituted or substituted repeat units with two different (DDQ) orientations similar to the case of strapped trimers (Figure S9 and S10). Boltzmann factors and percent weights of the configurations are determined as discussed above and are shown in Figure S9 and S10. In the case of both the linear trimers the DDQ is located on the middle repeat unit irrespective of the location of the substituents unlike the strapped trimers (Scheme 3). The percentage of the configuration with DDQ on the middle phenyl units is ca. 64% and 96% for PLP and LPL respectively. The binding energy of the most stable configurations of the linear trimers-DDQ complex is higher than that of the bare PPP-DDQ complex but lower than the strapped trimers. The computations confirm that DDQ has slight preference for the middle phenyl unit over the terminal phenyl unit of the PPP, whereas

DDQ has higher preference for the middle phenyl unit in the case of linear trimers irrespective of the location of the substituents. Only in the case of strapped trimers the DDQ is it directed toward the unsubstituted phenyl repeat units providing the control over the dopant location. Thus, strapped trimers exhibit strong binding interactions with DDQ compared to the analogous control molecules, and strapped trimers and therefore are useful to direct the DDQ to the desired location along the trimer by controlling the location of the adamantyl straps along the trimer backbone.

Since the binding energies of different configurations are close, each of them may coexist in the solution and contribute to the UV-vis absorption spectrum. So, the UV-vis absorption pattern for each configuration is computed and the contribution of each of these configurations to the UV-vis absorption spectrum is computed by multiplying each configurations' Boltzmann factor with the charge transfer peak oscillator strength (Tables 1-3). We are gratified to see that the simulated charge transfer peak positions are close, within 80 nm, to the experimentally observed charge transfer peak positions (Figure 11). The gap between the simulated and experimental charge transfer peak position are common in the literature.[54] The presence of simulated charge transfer peaks within the 80 nm of experimentally observed charge transfer
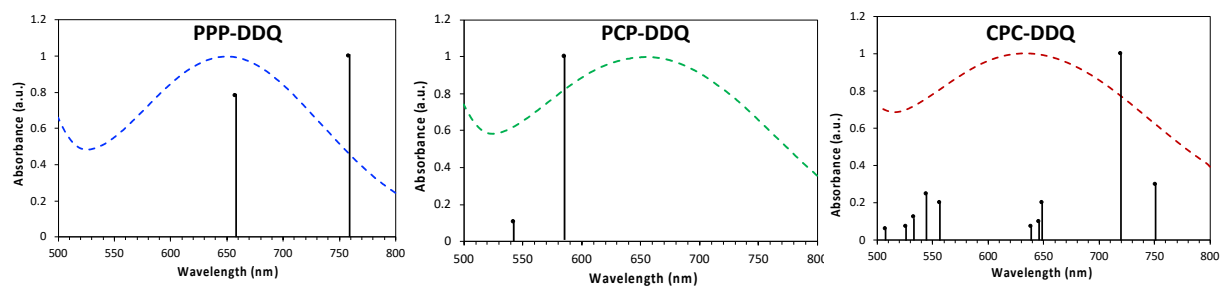
Figure 11. Experimental (dotted line) UV-Vis absorption spectra is overlaid with theoretical transitions (solid line) calculated from TD-DFT with CAM-B3LYP/6-311G**.

peak position gives confidence in the simulated DA configurations.

In the case of PPP the location of DDQ is driven by the thermodynamics of complexation and DDQ residing on the middle phenyl repeat unit is the highest contributing configuration. On the other hand, in the case of the strapped trimers, the presence of strapped repeat units makes some of the locations less favorable for DDQ to bind. The location of the DDQ is driven by the location of the strapped repeat unit(s) in addition to the thermodynamics of complexation. In the highest contributing configuration of PCP-DDQ system, unlike the PPP-DDQ system, DDQ is located on the terminal phenyl repeat units that have no strapped units but not on the middle phenyl repeat unit. In the highest contributing configuration of CPC-DDQ system, DDQ is also located on the non-strapped phenyl repeat unit, which is the middle phenyl repeat unit CPC. Even though not all the locations are available in strapped trimers, we are gratified to see that the available binding locations result in higher binding energy configurations as well as higher dopant ionization than that of the unmasked DA complex (PPP-DDQ). DDQ is directed towards the middle phenyl units in the case of linear trimers-DDQ complexes even though both the linear and strapped trimers contain similar type of substituents. This indicates that selectively masking a few of the repeat units along the trimer enhances the percentage of dopant ionization. Within the strapped trimers the percentage of dopant ionization depends on the location of the masked repeat units along the trimer and highlights the importance of controlling the DA configuration to realize higher dopant ionization. So far in the literature electronic rich/deficient substituents have been used to control the DA interaction strength and dopant ionization but there are no reports on controlling the DA configuration. Herein, we show that the cycloalkyl straps provide control over the DA configuration and enhance the dopant ionization. For thermoelectric device related

applications the high doping efficiency in thinfilms is required, our future work focuses toward this including the optical properties of the CT complexes in thinfilms.

Conclusions

It is known that masking the π-face of the polymers hinders interchain interactions as well as reduces photoinduced charge transfer from polymer to an acceptor. Herein, we show that by selectively masking the π-face of few repeat units in the donor, the location of the acceptor along the donor backbone as well as the DA binding strength is controllable. In case of the PPP donor, trimer with no strapped-repeat units, acceptor prefers to interact with the middle phenyl repeat unit and this more prevalent in the case of linear trimers. In the case of the strapped donors, the location of the acceptor is driven the by the location of the strapped repeat units in addition to the DA interaction strength. Based on DFT calculations DDQ prefers to interact with the non-strapped phenyls and the percentage of these configurations is at least 74%. Surprisingly, strapped donors result in stronger DA complexes with DDQ. More importantly, one of the strapped donors resulted in 59% higher ionization of DDQ compared to the unstrapped PPP donor. A comparison between strapped and linear trimers clearly indicated that the enhanced percentage of DDQ ionization is due to the selective masking of the pi-face. Thus, the π-face masking opens a new pathway to control the location of the dopant and obtain higher dopant ionization. Control over these factors has significant impact on the organic electronics that deals with both electronic rich and poor components including light emitting diodes, solar cells and thermoelectrics.

ASSOCIATED CONTENT

Supporting Information

Synthesis, characterization details, and DFT calculation details are included in the supplementary information.

AUTHOR INFORMATION

† These authors contributed equally.

Corresponding Author

* Corresponding author: N.G. (email: ng554@georgetown.edu);

Conflicts of Interest

There are no conflicts of interest to declare.

Author Contributions

J. S., A. M. and M. M. performed all the experimental work. J. S. performed all the computational studies. J.B. collected and solved the single crystal data. M. K. guided the computational studies. N. G. conceived the idea and guided the experimental work. All the authors are involved in data analysis and draft writing.

References

1.   Mityashin, A.; Olivier, Y.; Van Regemorter, T.; Rolin, C.; Verlaak, S.; Martinelli, N. G.; Beljonne, D.; Cornil, J.; Genoe, J.; Heremans, P., Unraveling the mechanism of molecular doping in organic semiconductors. *Adv. Mater.* **2012,** *24* (12), 1535-9.

2.   Mendez, H.; Heimel, G.; Winkler, S.; Frisch, J.; Opitz, A.; Sauer, K.; Wegner, B.; Oehzelt, M.; Rothel, C.; Duhm, S.; Tobbens, D.; Koch, N.; Salzmann, I., Charge-transfer crystallites as molecular electrical dopants. *Nat. Commun.* **2015,** *6*, 8560.

3.   Venkataraman, D.; Yurt, S.; Venkataraman, B. H.; Gavvalapalli, N., Role of Molecular Architecture in Organic Photovoltaic Cells. *J. Phys. Chem. Lett.* **2010,** *1*, 947-958.

4.   Lee, S.; Chenard, E.; DGray, D. L.; Moore, J. S., Synthesis of Cycloparaphenyleneacetylene via Alkyne Metathesis: C_{70} Complexation and Copper-Free Triple Click Reaction. *J. Am. Chem. Soc.* **2016,** *138*, 13814-13817.

5.   Du, Y.; Lovell, H. B.; Lirette, F.; Morin, J.-F.; Plunkett, K. N., Electron Acceptors Based on Cyclopentannulated Anthanthrenes. *J. Org. Chem.* **2021,** *86*, 1456-1461.

6.   Lu, Y.; Yu, Z. D.; Liu, Y.; Ding, Y. F.; Yang, C. Y.; Yao, Z. F.; Wang, Z. Y.; You, H. Y.; Cheng, X. F.; Tang, B.; Wang, J. Y.; Pei, J., The Critical Role of Dopant Cations in Electrical Conductivity and Thermoelectric Performance of n-Doped Polymers. *J. Am. Chem. Soc.* **2020,** *142* (36), 15340-15348.

7.   Wang, S.; Ruoko, T. P.; Wang, G.; Riera-Galindo, S.; Hultmark, S.; Puttisong, Y.; Moro, F.; Yan, H.; Chen, W. M.; Berggren, M.; Muller, C.; Fabiano, S., Sequential Doping of Ladder-Type Conjugated Polymers for Thermally Stable n-Type Organic Conductors. *ACS Appl. Mater. Interfaces* **2020,** *12* (47), 53003-53011.

8.   Yoon, S. E.; Kang, Y.; Noh, S. Y.; Park, J.; Lee, S. Y.; Park, J.; Lee, D. W.; Whang, D. R.; Kim, T.; Kim, G. H.; Seo, H.; Kim, B. G.; Kim, J. H., High Efficiency Doping of Conjugated Polymer for Investigation of Intercorrelation of Thermoelectric Effects with Electrical and Morphological Properties. *ACS Appl. Mater. Interfaces* **2020,** *12* (1), 1151-1158.

9.   Zapata-Arteaga, O.; Perevedentsev, A.; Marina, S.; Martin, J.; Reparaz, J. S.; Campoy-Quiles, M., Reduction of the Lattice Thermal Conductivity of Polymer Semiconductors by Molecular Doping. *ACS Energy Lett.* **2020,** *5* (9), 2972-2978.

10.   Bubnova, O.; Crispin, X., Towards polymer-based organic thermoelectric generators. *Energy Environ. Sci.* **2012,** *5* (11), 9345.

11.   Ma, T.; Dong, B. X.; Grocke, G. L.; Strzalka, J.; Patel, S. N., Leveraging Sequential Doping of Semiconducting Polymers to Enable Functionally Graded Materials for Organic Thermoelectrics. *Macromolecules* **2020,** *53* (8), 2882-2892.

12.   Untilova, V.; Biskup, T.; Biniek, L.; Vijayakumar, V.; Brinkmann, M., Control of Chain Alignment and Crystallization Helps Enhance Charge Conductivities and Thermoelectric Power Factors in Sequentially Doped P3HT:F4TCNQ Films. *Macromolecules* **2020,** *53* (7), 2441-2453.

13.   Untilova, V.; Hynynen, J.; Hofmann, A. I.; Scheunemann, D.; Zhang, Y.; Barlow, S.; Kemerink, M.; Marder, S. R.; Biniek, L.; Muller, C.; Brinkmann, M., High Thermoelectric Power Factor of Poly(3-hexylthiophene) through In-Plane Alignment and Doping with a Molybdenum Dithiolene Complex. *Macromolecules* **2020,** *53* (15), 6314-6321.

14.   Meng, B.; Liu, J.; Wang, L., Recent development of n-type thermoelectric materials based on conjugated polymers. *Nano Mater. Sci.* **2021,** *3*, 113-123.

15.   Patel, S. N.; Glaudell, A. M.; Peterson, K. A.; Thomas, E. M.; O'Hara, K. A.; Lim, E.; Chabinyc, M. L., Morphology Controls the Thermoelectric Power Factor of a Doped Semiconducting Polymer. *Sci. Adv.* **2017,** *3* (6).

16.   Park, J.; Yoon, S. E.; Kang, Y.; Lee, I.; Kim, J. H.; Kim, B.-G., Doping characteristics of isoindoloindole-based conjugated polymer toward robust transformable organic conductor. *Org. Electron.* **2019,** *75*, 105435.

17.   Chaudhuri, S.; Mohanan, M.; Willems, A. V.; Bertke, J. A.; Gavvalapalli, N., B-Strand inspired bifacial pi-conjugated polymers. *Chem. Sci.* **2019,** *10*, 5976-5982.

18.   Li, Y.; Jia, Z.; Xiao, S.; Liu, H.; Li, Y., A Method for Controlling the Synthesis for Stable Twisted Two-Dimensional Conjugated Molecules. *Nat. Commun.* **2016,** *7*.

19.   Zheng, T.; Cai, Z.; Ho-Wu, R.; Yau, S. H.; Shaparov, V.; Goodson, T. I.; Yu, L., Synthesis of Ladder-Type Thienoacenes and their Electronic and Optical Properties. *J. Am. Chem. Soc.* **2016,** *138*, 868-875.

20.   Leventis, A.; Royakkers, J.; Rapidis, A. G.; Goodeal, N.; Corpinot, M. K.; Frost, J. M.; Bučar, D.-K.; Blunt, M. O.; Cacialli, F.; Bronstein, H., Highly Luminescent Encapsulated Narrow Bandgap Polymers Based on Diketopyrrolopyrrole. *J. Am. Chem. Soc.* **2018,** *140* (5), 1622-1626.

21.   Royakkers, J.; Bronstein, H., Macrocyclic Encapsulated Conjugated Polymers. *Macromolecules* **2021,** *54* (3), 1083-1094.

22.   Pan, C.; Sugiyasu, K.; Wakayama, Y.; Sato, A.; Takeuchi, M., Thermoplastic Fluorescent Conjugated Polymers: Benefits of Preventing π-π Stacking. *Angew. Chem. Int. Ed.***2013,** *52* (41), 10775-10779.

23.   Giovannitti, A.; Nielsen, C. B.; Rivnay, J.; Kirkus, M.; Harkin, D. J.; White, A. J. P.; Sirringhaus, H.; Malliaras, G. G.; McCulloch, I., Sodium and Potassium Ion Selective Conjugated Polymers for Optical Ion Detection in Solution and Solid State. *Adv. Funct. Mater.* **2015,** *26* (4), 514-523.

24.   Morgan, B. P.; Gilliard, R. J.; Loungani, R. S.; Smith, R. C., Poly(p -phenylene ethynylene) Incorporating Sterically Enshrouding m -Terphenyl Oxacyclophane Canopies. *Macromol. Rapid Commun.* **2009,** *30* (16), 1399-1405.

25.   Cacialli, F.; Wilson, J. S.; Michels, J. J.; Daniel, C.; Silva, C.; Friend, R. H.; Severin, N.; Samori, P.; Rabe, J. P.; O'Connell, M. J.; Taylor, P. N.; Anderson, H. L., Cyclodextrin-threaded conjugated polyrotaxanes as insulated molecular wires with reduced interstrand interactions. *Nat. Mater.* **2002,** *1* (3), 160-4.

26.   Frampton, M. J.; Anderson, H. L., Insulated molecular wires. *Angew. Chem. Int. Ed. Engl.* **2007,** *46* (7), 1028-64.

27.   Fiesel, R.; Huber, J.; Apel, U.; Enkelmann, V.; Hentschke, R.; Scherf, U.; Cabrera, K., Novel chiral poly(para-phenylene) derivatives containing cyclophane-type moieties. *Macromol. Chem. Phys.* **1997,** *198* (9), 2623-2650.

28.   Schluter, A. D.; Loffler, M.; Enkelmann, V., SYNTHESIS OF A FULLY UNSATURATED ALL-CARBON LADDER POLYMER. *Nature* **1994,** *368* (6474), 831-834.

29.   Morisaki, Y.; Chujo, Y., Cyclophane-containing polymers. *Prog. Polym. Sci.* **2008,** *33* (3), 346-364.

30.   Das, M. K.; Hameed, F.; Lillis, R.; Gavvalapalli, N., A twist in the non-slanted H-mers to control π-conjugation in 2-dimensions and optical properties. *Mater. Adv.* **2020,** *1* (8), 2917- 2925.

31.   Lillis, R.; Thomas, M. R.; Mohanan, M.; Gavvalapalli, N., Enhancing Insulated Conjugated Polymer Fluorescence Quenching by Incorporating Dithia[3.3]paracyclophanes. *Macromolecules* **2021,** *54*, 3112-3119.

32.   Frisch, M. J.; Trucks, W. G.; Schlegl, H. B.; Scuseria, G. E.; Robb, M. A.; Cheeseman, J. R.; Scalamani, B. V.; Peterson, G. A.; Nakatsuji, H.; Li, X.; Caricato, M.; Marenich, A. V.;

Bloino, J.; Jankesko, B. G.; Gomperts, R.; Mennucci, B.; Hratchian, H. P.; Ortiz, J. V.; Izmaylov, A. F.; Sonneberg, J. L.; Williams-Young, D.; Ding, F.; Lipparini, F.; Egidi, F.; Goings, J.; Peng, B.; Petrone, A.; Henderson, T.; Ranasinghe, D.; Zakrzewski, V. G.; Gao, J.; Rega, N.; Zheng, G.; Liang, W.; Hada, M.; Ehara, M.; Toyota, K.; Fukuda, R.; Hasegawa, J.; Ishida, M.; Nakajima, T.; Honda, Y.; Kitao, O.; Nakai, H.; Vreven, T.; Throssell, K.; Montgomery, J. A. J.; Peralta, J. E.; Ogliaro, F.; Bearpark, M. J.; Heyd, J. J.; Brothers, E. N.; Kudin, K. N.; Staroverov, V. N.; Keith, T. A.; Kobayashi, R.; Normand, J.; Raghavachari, K.; Rendell, A. P.; Burant, J. C.; Iyengar, S. S.; Tomasi, J.; Cossi, M.; Millam, J. M.; Klene, M.; Adamo, C.; Cammi, R.; Ochterski, J. W.; Martin, R. L.; Mokokuma, K.; Farkas, O.; Foresman, J. B.; Fox, D. J. *Gaussian 16, Revision A.03*, Guassian, Inc.: Wallingford, CT, 2016.

33.   Adamo, C.; Jacquemin, D., The calculations of excited-state properties with Time-Dependent Density Functional Theory. *Chem. Soc. Rev.* **2013,** *42* (3), 845-56.

34.   Maitra, N. T., Charge transfer in time-dependent density functional theory. *J. Phys. Condens. Matter* **2017,** *29* (42), 423001.

35.   Das, M. K.; Hameed, F.; Lillis, R.; Gavvalapalli, N., A Twist in the non-slanted H-Mers to control pi-conjugation in 2-dimensions and optical properties. *Mater. Adv.* **2020,** *1*, 2917-2925.

36.   Chipman, D. M.; Prebenda, M. F., Structures and Fundamental Vibrations of p-Benzoquinone and p-Benzosemiquinone Radical Anion from ab initio Calculations. *J. Phys. Chem.* **1986,** *90*, 5557-5560.

37.   Kawabata, K.; Osaka, I.; Sawamoto, M.; Zafra, J. L.; Mayorga Burrezo, P.; Casado, J.; Takimiya, K., Dithienyl Acenedithiophenediones as New pi-Extended Quinoidal Cores: Synthesis and Properties. *Chemistry* **2017,** *23* (19), 4579-4589.

38.   Sharma, K.; Sharma, S. P.; Lahiri, S. C., Spectrophotometric, Fourier transform infrared spectroscopic and theoretical studies of the charge-transfer complexes between methyldopa [(S)-2 amino-3-(3,4-dihydroxyphenyl)-2-methyl propanoic acid] and the acceptors (chloranilic acid, o-chloranil and dichlorodicyanobenzoquinone) in acetonitrile and their thermodynamic properties. *Spectrochim. Acta. A.: Mol. Biomol. Spectrosc.* **2012,** *92*, 212-24.

39.   Kalimuthu, P.; Sivanesan, A.; John, S. A., Charge-transfer interaction of aromatic thiols with 2,3-dichloro-5,6-dicyano-p-benzoquinone: spectral and quantum mechanical studies. *J. Phys. Chem. A* **2007,** *111* (48), 12086-92.

40.   Srivastava, R. D.; Prasad, G., Charge Transfer Interaction between 2,3-Dichloro-5,6-dicyano-p-benzoquinone and substituted benzenes. *Bull. Chem. Soc. Jpn* **1970,** *43*, 1611-1614.

41.   Foster, R.; Thomson, T. J., Interaction of Electron Acceptors with Base. *Trans. Faraday Soc.* **1962,** *58*, 860-868.

42.   Miller, J. S.; Krusic, P. J.; Dixon, D. A.; Reiff, W. M.; Zhang, J. H.; Anderson, E. C.; Epstein, A. J., Radical Anion Salts of 2,3-Dichloro-5,6-dicyanbenzoquinone and Metallocenes. A Reexamination of Their Magnetic and Spectroscopic Properties. *J. Am. Chem. Soc.* **1986,** *108*, 4459-4466.

43.   Harada, M.; Tanioka, M.; Muranaka, A.; Aoyama, T.; Kamino, S.; Uchiyama, M., A Remarkably Air Stable Quinodimethane Radical Cation. *Chem. Commun.* **2020,** *56*.

44.   Wan, J.; Ferriera, A.; Xia, W.; Chow, C. H.; Takechi, K.; Kamat, P. V.; Jones, G. I.; Vullev, V. I., Solvent dependence of the charge-transfer properties of a quarterthiophene-anthraquinone dyad. *J. Photochem. Photobiol., A* **2008,** *197*, 364-374.

45.   Zhang, Y.; Yang, X.; Wang, W.; Wang, X.; Sun, L., DDQ as an effective p-type dopant for the hole transport material X1 and its application in stable solid-state dye-sensitized solar cells. *J. Energy Chem.* **2018,** *27*, 413-418.

46.   Liu, H.; Cui, M.; Dang, C.; Wen, W.; Wang, X.; Xie, L., Two-Dimensional WSE$_2$/Organic Acceptor Hybrid Nonvolatile Memory Devices Based on Interface Charge Trapping. *ACS Appl. Mater. Interfaces* **2019,** *11*, 34424-34429.

47.   Hu, P.; Ma, L.; Tan, K. J.; Jiang, H.; Wei, F.; Yu, C.; Goetz, K. P.; Jurchescu, O. D.; McNeil, L. E.; Gurzadyan, G. G.; Kloc, C., Solvent-Dependent Stoichiometry in Perylene–7,7,8,8-Tetracyanoquinodimethane Charge Transfer Compound Single Crystals. *Cryst. Growth Des.* **2014,** *14* (12), 6376-6382.

48.   Vermeulen, D.; Zhu, L. Y.; Goetz, K. P.; Hu, P.; Jiang, H.; Day, C. S.; Jurchescu, O. D.; Coropceanu, V.; Kloc, C.; McNeil, L. E., Charge Transport Properties of Perylene–TCNQ Crystals: The Effect of Stoichiometry. *J. Phys. Chem. C* **2014,** *118* (42), 24688-24696.

49.   Jiang, H.; Hu, P.; Ye, J.; Zhang, K. K.; Long, Y.; Hu, W.; Kloc, C., Tuning of the degree of charge transfer and the electronic properties in organic binary compounds by crystal engineering: a perspective. *J. Mater. Chem. C* **2018,** *6* (8), 1884-1902.

50.	Hu, P.; Du, K.; Wei, F.; Jiang, H.; Kloc, C., Crystal Growth, HOMO–LUMO Engineering, and Charge Transfer Degree in Perylene-FxTCNQ (x = 1, 2, 4) Organic Charge Transfer Binary Compounds. *Cryst. Growth Des.* **2016,** *16* (5), 3019-3027.

51.	Mahns, B.; Kataeva, O.; Islamov, D.; Hampel, S.; Steckel, F.; Hess, C.; Knupfer, M.; Büchner, B.; Himcinschi, C.; Hahn, T.; Renger, R.; Kortus, J., Crystal Growth, Structure, and Transport Properties of the Charge-Transfer Salt Picene/2,3,5,6-Tetrafluoro-7,7,8,8-tetracyanoquinodimethane. *Cryst. Growth Des.* **2014,** *14* (3), 1338-1346.

52.	Dobrowolski, M. A.; Garbarino, G.; Mezouar, M.; Ciesielski, A.; Cyrański, M. K., Structural diversities of charge transfer organic complexes. Focus on benzenoid hydrocarbons and 7,7,8,8-tetracyanoquinodimethane. *CrystEngComm* **2014,** *16* (3), 415-429.

53.	Ganesan, V.; Rosokha, S. V.; Kochi, J. K., Isolation of the Latent Precursor Complexin Electron-Transfer Dynamics. Intermolecular Association and Self-Exchange with Acceptor Anion Radicals. *J. Am. Chem. Soc.* **2003,** *125*, 2559-2571.

54.	Strahan, J.; Popere, B. C.; Khomein, P.; Pointer, C. A.; Martin, S. M.; Oldacre, A. N.; Thayumanavan, S.; Young, E. R., Modulating absorption and charge transfer in bodipy-carbazole donor-acceptor dyads through molecular design. *Dalton Trans.* **2019,** *48* (23), 8488-8501.